THE ASTROPHYSICAL JOURNAL, 393:134–148, 1992 July 1

THE X-RAY SPECTRA OF GALAXIES. II. AVERAGE SPECTRAL PROPERTIES AND EMISSION MECHANISMS

D.-W. KIM
Chungnam National University, Daejeon 305-764, South Korea; and Harvard-Smithsonian Center for Astrophysics, 60 Garden Street, Cambridge, MA 02138
G. FABBIANO
Harvard-Smithsonian Center for Astrophysics, 60 Garden Street, Cambridge, MA 02138
AND
G. TRINCHIERI
Osservatorio Astrofisico di Arcetri, Largo E. Fermi 5, 50125 Firenze, Italy; and Harvard-Smithsonian Center for Astrophysics, 60 Garden Street, Cambridge, MA 02138
Received 1991 September 25; accepted 1992 January 9

ABSTRACT

We have systematically investigated the X-ray spectra of normal galaxies, by using the Imaging Proportional Counter (IPC) data in the *Einstein* data base. We find that on the average the X-ray emission temperature of spirals is higher than that of ellipticals. This is consistent with our understanding that accreting binaries are a major source of X-rays in spirals, while a hot interstellar medium (ISM) is present in ellipticals. The X-ray spectra of Sa galaxies are intermediate between those of ellipticals and spirals, suggesting that these galaxies contain hot gaseous emission as well as emission from accreting binaries. We confirm that the X-ray to optical ratio is an important indicator of the presence of a hot gaseous component in early-type galaxies. In particular we find that the emission temperature becomes higher with a decreasing X-ray to optical luminosity ratio in E and S0 galaxies. This result is what we would expect if the emission of X-ray faint early-type galaxies consists of a large evolved stellar component, while the gaseous emission becomes dominant in X-ray brighter galaxies. The group with the lowest L_X/L_B does not follow this trend. In these galaxies we find a *very soft* ($kT \sim 0.2$ keV) X-ray component, amounting to about half the total X-ray emission, in addition to the hard X-ray component. Possible explanations for this component include the integrated emission of M stars and a relatively cool ISM. A *very soft* component is also found in several spiral galaxies. This result may indicate that some spirals contain hot gaseous components similar to those seen in NGC 253 and M82.

Subject headings: galaxies: elliptical and lenticular, cD — galaxies: spiral — radiation mechanisms: miscellaneous — X-rays: galaxies

1. INTRODUCTION

Based on the results from the *Einstein Observatory* (Giacconi et al. 1979), it is now known that normal galaxies of all morphological types are sources of X-ray emission with luminosities in the range of 10^{38}–10^{42} ergs s^{-1} (see Fabbiano 1989 for a review). The imaging data and the results of the spectral fits of a relatively small number of galaxies have suggested that different sources are responsible for the X-ray emission in galaxies of different morphological types. While in spiral galaxies accreting binaries are a major source of X-ray emission (see Fabian 1981; Helfand 1984; Fabbiano & Trinchieri 1985, 1987), in bright elliptical galaxies hot gaseous emission can be the dominant source of X-rays (Forman, Jones, & Tucker 1985; Trinchieri & Fabbiano 1985; Canizares, Fabbiano, & Trinchieri 1987). Supernova remnants or masssive young stars may dominate in blue starburst galaxies, together with emission from outflowing gaseous plumes in some cases (Fabbiano, Feigelson, & Zamorani 1982; Stewart et al. 1982; Watson, Stanger, & Griffiths 1984; Fabbiano & Trinchieri 1984; Fabbiano 1988b; Fabbiano, Heckman, & Keel 1990).

The purpose of this paper is to study the average spectral properties of reasonably large samples of galaxies of different types and to use these results to constrain the X-ray emission mechanisms. To this end we use the sample of 127 galaxies detected with the *Einstein* IPC (see Fabbiano, Kim, & Trinchieri 1992), whose spectral parameters and/or X-ray colors have been tabulated by Kim, Fabbiano, & Trinchieri (1992, hereafter Paper I). Most of these galaxies were not detected with enough statistics to yield meaningful spectral parameters, when analyzed singly. To overcome this problem, we have studied the distribution of X-ray colors, and we have derived and compared combined spectra for given classes of galaxies. The analysis methods are described and justified in § 2. The sample selection is discussed in § 3.

First, we investigate the differences in the average X-ray spectra of galaxies of different morphological types (§ 4). In particular, we examine the average spectral properties of spiral and elliptical galaxies, and we take a closer look at S0 and Sa galaxies, intermediate in disk-to-bulge ratio, to determine the relative importance of stellar sources and hot gaseous ISM in their X-ray emission.

Second, we address the question whether E and S0 galaxies with relatively faint X-ray emission retain a hot gaseous ISM as do X-ray luminous elliptical galaxies (§ 5). If the spectra of less luminous ellipticals differ from those of the bright galaxies, this may imply a global difference between the two subsamples in the process of formation and evolution. If early-type galaxies with hot gaseous components can be properly selected by their X-ray spectra, they can then be used to further investigate the implications of hot gas for the study of cooling flows and dark matter. The presence or absence of a hot ISM in different kinds

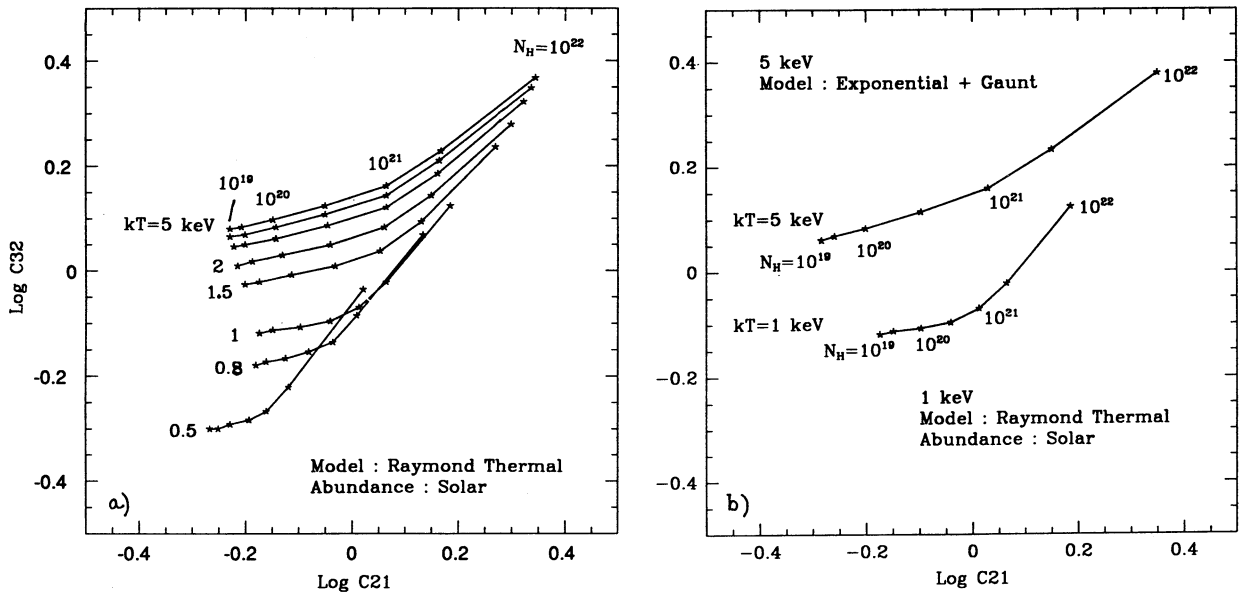

FIG. 1.—X-ray color-color plot of model predictions. (*a*) Raymond thermal emission models with solar abundance, for kT ranging from 0.5 to 5. keV and N_H ranging from 10^{19}–10^{22} cm^{-2}. (*b*) The lower line is for a Raymond thermal emission model with $kT = 1$ keV and solar abundances. The upper line is for bremsstrahlung emission with $kT = 5$ keV.

of early-type galaxies has been debated, but could not be solved with the "traditional" spectral analysis techniques because of limited signal-to-noise ratio (e.g., Fabbiano 1989; Fabbiano, Gioia, & Trinchieri 1989; Canizares et al. 1987).

Third, we examine galaxies whose spectral parameters differ significantly from the average spectral parameters of their given classes. In particular, we discuss the presence of very soft emission components in both elliptical and spiral galaxies. We also investigate possible spectral signatures of inclination in spiral galaxies (§§ 5 and 6).

2. ANALYSIS METHODS

In Paper I we gave the results of two-parameter spectral fits to the IPC data for 43 galaxies, and we tabulated X-ray colors for 127 galaxies. Here we will use these X-ray colors to investigate average spectral properties. We will also use composite X-ray spectra, obtained by summing the spectral count distributions of many galaxies. IPC counts were transposed from the instrumental pulse height (PH) bins to the gain-corrected pulse invariant (PI) bins as part of the Rev-1B IPC reprocessing (Harnden et al. 1984). This procedure makes a correction for the effect of variations of the instrumental gain and puts the energy boundaries of the bins on a common scale. PI bins were used to derive colors and composite spectra.[1]

2.1. *X-Ray Colors*

The definition of X-ray colors was introduced in Paper I. These colors were derived by dividing the gain-corrected IPC spectral band into three parts and calculating the following ratios:

$$\text{C21} = \text{counts(0.8–1.4 keV)/counts(0.2–0.8 keV)} ,$$

$$\text{C32} = \text{counts(1.4–3.5 keV)/counts(0.8–1.4 keV)} .$$

In Figure 1*a*, we plot the X-ray colors predicted by Raymond thermal models with solar abundances for kT ranging from 0.5 to 5 keV and $N_H = 10^{19}$–10^{22} cm^{-2}. This figure shows that there is little difference in colors for $kT \geq 3$ keV. This is due to the poor sensitivity of the mirror/IPC response at the high energies. Figure 1*b* shows the X-ray colors for a 1 keV Raymond model (and varying N_H), and for a 5 keV bremsstrahlung model (exponential plus Gaunt; this model has been used for accreting binary sources). The latter follows the same track as the 5 keV Raymond model, but tends to give higher values of N_H for the same colors. This difference is due to the different shape of the continuum in the two models at the low energies, and to a different treatment of the Gaunt factor. The Gaunt factor is explicitly calculated in the Raymond model, while an average value is used for the simple exponential model. We will use Figure 1*b* as a reference against which to compare our data. As can be seen from Figure 1, the first X-ray color, C21, is sensitive primarily to the hydrogen column density (N_H), while the second color, C32, is sensitive to the emission temperature (kT), except for very large column densities. For a large absorbing column density ($N_H \sim 10^{22}$ cm^{-2}), a 1 keV spectrum looks hard due to strong absorption even above 0.8 keV. As we will show later, X-ray colors provide reasonable estimates of the average spectral parameters for subsamples of galaxies, even if the uncertainties on the colors of a single faint galaxy are large.

2.2. *Composite Spectra*

As a second estimate of average properties, we have combined the counts in PI channels for given subsamples of galaxies and generated a representative spectrum for the sub-

[1] After completing this work, we discovered a long-hidden bug in the Rev-1B IPC processing software, which may result in an erroneous estimate of the gain used for assigning counts to PI bins. We have therefore checked all the PI spectral distributions of all the 127 galaxies by comparing them against those derived by the off-line spectral software, which uses PH binned data and corrects for the instrumental gain. The off-line software is not affected by the bug. In all cases the distributions were compatible within the errors; therefore our work is not affected by the processing bug. Moreover, any gain variation would be within the margin discussed in § 2.3.

sample. We have then used these distributions of PI channels for direct comparisons, to calculate "composite" colors, and to perform model fits.

Generating a composite spectrum simply by adding the PI counts from different observations might, however, bias our results in the sense of giving naturally more weight to the data with a higher signal-to-noise ratio. In order to make sure that a few very bright objects do not dominate the combined spectra, we have in all cases redone our analysis by excluding strong sources and confirmed that the results do not change significantly (see below for each case).

2.3. *Effect of IPC Gain Uncertainty*

Although counts are assigned to PI bins taking into account the average IPC gain at a given time, there is still some residual uncertainty, especially for off-axis sources. The "true" value of the IPC gain could differ by as much as ± 1 from the nominal value. This corresponds to an uncertainty of $\pm \frac{1}{2}$ PH channel on the channel corresponding to the 1.5 keV Al calibration line.

To estimate the effect of this uncertainty on the combined average colors and on the PI-binned composite spectra, we have performed the following experiment. We have used two representative input spectra: a soft spectrum with $kT = 1$ keV, and a hard spectrum with $kT = 5$ keV, both with $N_H = 3 \times 10^{20}$ cm^{-2}. The 1 keV spectrum is typical of bright early-type galaxies (Paper I and references therein) and, as we will show later, is also a good representation of the average spectrum of the early-type sample discussed here, which is dominated by X-ray bright galaxies. The 5 keV spectrum is a reasonable fit to the data of bright spirals (Paper I), and a hard spectrum is also representative of the average spectral properties of our spiral sample (see below). Given the spectral response of the mirror/IPC, it is not meaningful to try to discriminate between different kT values above ~ 3 keV (see Fig. 1*a*). The adopted value of N_H is in the range of the results of Paper I. From each of these input spectra we have then generated two sets of "observed" spectra (A and B as explained below), with randomly assigned net counts in the range of 50–150 counts for each simulated spectrum. To reflect the spread of the IPC gain present in our observations, we have used three "nominal" gain values (13, 15.6, and 18) for each set, and we have generated 36, 76, and 47 "observed" spectra (reflecting the number of observations of galaxies in each gain bin: 159 observations for 127 galaxies), by convolving the data with the IPC response for a given gain value. For set A we have generated "observed" spectra using these nominal gain values. For set B, we have used randomly generated gain values within ± 1 of the nominal gain, to simulate the uncertainty in the gain.

We have then computed colors for the composite 1 and 5 keV A spectra and for the randomly generated (as explained above) sets of composite B spectra. We find very good agreement. The spread in colors for a set of 100 composite B spectra is shown in Figure 2*a*, which shows that the X-ray colors are not affected by the uncertain in the IPC gain. The composite colors for the A spectra are within the distribution of the B spectra colors. We then performed two-parameter fits on the two composite spectra obtained by adding the source PI counts of the two sets of A–1 keV and A–5 keV spectra, and on randomly generated (as explained above) composite B–1 keV and B–5 keV spectra. The best-fit kT and N_H are shown in Figure 2*b* and 2*c* for the A spectra and for sets of 100 composite B spectra. It is clear from the figure that the uncertainty on the gain does not affect significantly our results. In the case of a hard spectrum it introduces an uncertainty on kT of ± 1 keV; in the case of a soft spectrum, it introduces a very small uncertainty in the determination of N_H.

The results of these simulations show that differences in the average colors of subsamples of galaxies can be used as a diagnostic of spectral differences. Moreover, spectral parameters obtained from the spectral fits of composite spectra are indicative of the intrinsic average spectral parameters for the sample. If the galaxies in one of our samples have intrinsically soft spectra, the analysis of the composite spectrum will give low values of kT, representative of the true emitted spectrum. If the analysis of a composite spectrum gives high values of kT, the intrinsic emitted spectra must be hard, although the value of the average intrinsic kT could be somewhat uncertain.

Moreover, the range of gains (and uncertainties) is similar for the different subsamples used in this paper, which were all chosen on the basis of astronomical properties of which the IPC could not have any "knowledge." Therefore spectral differences are not likely to arise from instrumental problems.

3. SAMPLE SELECTION

The galaxies used for this paper are a subsample of the 127 galaxies for which colors are listed in Paper I. Galaxies which have ambiguous sources (i.e., the X-ray emission could be due to interlopers) or were partly hidden by the detector supporting structure have been excluded. We also omit observations for which the X-ray color is unreasonable (negative counts in one band or very large error, $>60\%$). These sources have small net counts so that small background fluctuations (caused by the presence of nearby sources, extended emission, etc.) might cause these odd or ill-determined colors (Paper I). The LMC, SMC, M31, M33, and M101, which have been analyzed in detail elsewhere (see § 4.1 and Paper I and references therein), were not included in this study. We also excluded M81, whose X-ray emission is dominated by a nuclear source (Fabbiano 1988a). This resulted in 37 E and S0 galaxies and 48 spirals.

This sample is by no means complete. However, it should be representative of the spectral properties of different types of galaxies, because the properties we seek to explore do not enter in our selection criteria. Our selection might have excluded a few galaxies with extreme spectra, that is, galaxies detected only in the soft or in the hard channels, because we pose minimum significance requirements on both X-ray colors. We have identified eight such galaxies, seven of which are spirals. All of these galaxies are detected with relatively few counts, so that statistically they would have a small weight. The fact that only one elliptical is in this category means that our conclusions on early-type galaxies are not affected by this bias. As for the spirals, the significant colors have typically average values for these galaxies, except in the case of NGC 4826, which has a very low value of C21 (C21 $= 0.39 \pm 0.14$), indicative of very soft emission. This galaxy should probably be added to those discussed in § 6.1.

4. SPECTRAL PROPERTIES AND MORPHOLOGICAL TYPE

4.1. *Elliptical and Spiral Galaxies*

Published papers on X-ray observations of bright galaxies have suggested different emission mechanisms for spiral and elliptical galaxies (see review in Fabbiano 1989). The X-ray emission in spiral galaxies appears to be dominated by a collection of discrete evolved stellar sources, mainly accreting

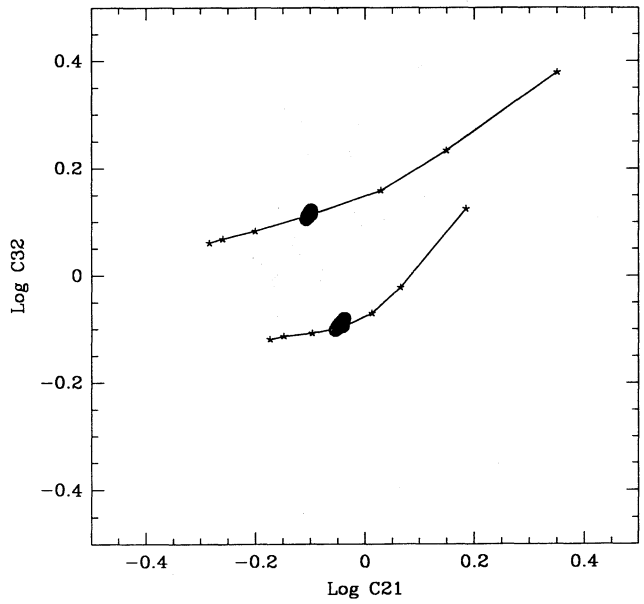

FIG. 2a

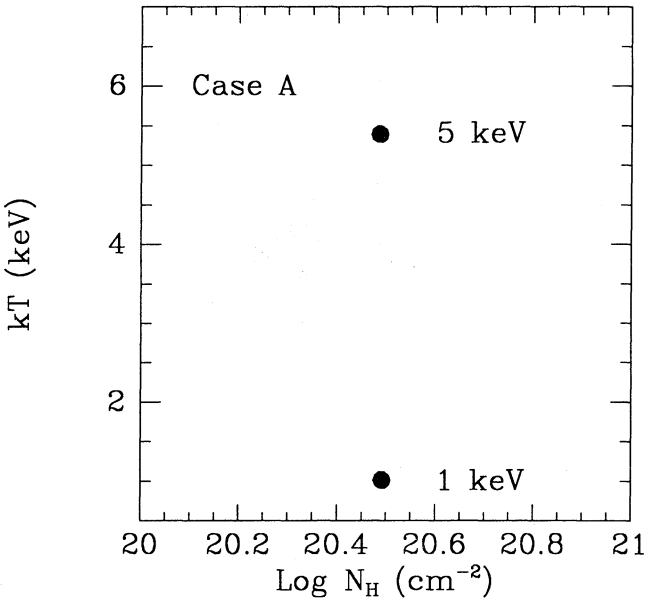

FIG. 2b

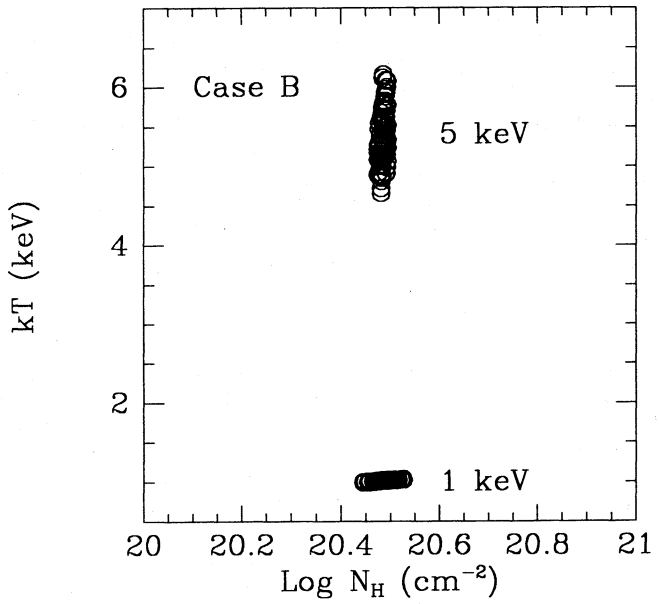

FIG. 2c

FIG. 2.—(*a*) Simulated average colors for a 5 keV and a 1 keV input spectra with gain error of up to ±1 on each composite spectrum. (*b*) Best-fit parameters (kT and N_H) for a 5 keV and a 1 keV composite spectrum with nominal gains (*see text*); (*c*) The same for randomly simulated composite spectra with gain errors of ±1 on each component spectrum.

binaries, while in bright elliptical galaxies a hot gaseous component is responsible for the X-ray emission. The two-parameter spectral fits to thermal emission models of galaxies detected with ≥300 IPC net counts on the average support these earlier conclusions. Paper I shows that among the elliptical galaxies, NGC 499, 4406, 4472, 4552, 4636, 4649, 5044, 5846, and 7619 have kT of order of ~1 keV. For most spirals, the contours are usually open toward higher temperatures. This is because the mirror/IPC sensitivity drops significantly beyond ~4 keV. The spectral parameters of NGC 1097 and NGC 4579 are relatively well confined with kT of 2–3 keV. Higher emission temperatures are also reported for the nearby, well-studied spiral galaxies, M31 (Fabbiano, Trinchieri, & Van Speybroeck 1987; Trinchieri & Fabbiano 1991), M33 (Trinchieri, Fabbiano, & Perês 1988), and M101 (Trinchieri, Fabbiano, & Romaine 1990).

Using our larger sample, we can confirm and generalize these results. In Figure 3 X-ray colors are plotted for 37 elliptical and S0 galaxies and 48 spirals. Are the two distributions of Figure 3 different, or are they likely to originate from the same parent population? In Figure 4 we plot the means of the two distributions with their statistical errors (circles). We also plot (squares) the means weighted by the inverse square of the errors. This gives more weight to galaxies detected with more counts. In both cases, the means are well separated within the errors and suggest that spiral galaxies have on the average higher emission temperatures than ellipticals. The consistency of the two methods also indicates that the result is not due to a small number of very bright objects.

In Figure 5 we show the cumulative probability distributions (Kolmogorov-Smirnov test) of the X-ray colors for the two samples. It is clear that the distributions of C32 (~temperature) differ, while the distributions of C21 (~N_H) are similar. Student's t-test gives probabilities of 0.59 and 4.7×10^{-4} that the two distributions are from the same parent population for C21 and C32, respectively.

The above tests, however, consider only the distribution of X-ray colors, disregarding the statistical error associated with each color. Because the errors of individual estimates can be considerable, we have performed a simulation to see how strongly these uncertainties can affect our results. We have distributed 100 points for each galaxy according to a Gaussian function with a given mean color and standard deviation comparable to the measured error bar. We have then selected randomly one out of these 100 points for each galaxy and estimated a mean for each simulation. Figure 6 shows the distribution of the estimated means for 30 simulations. The X-ray

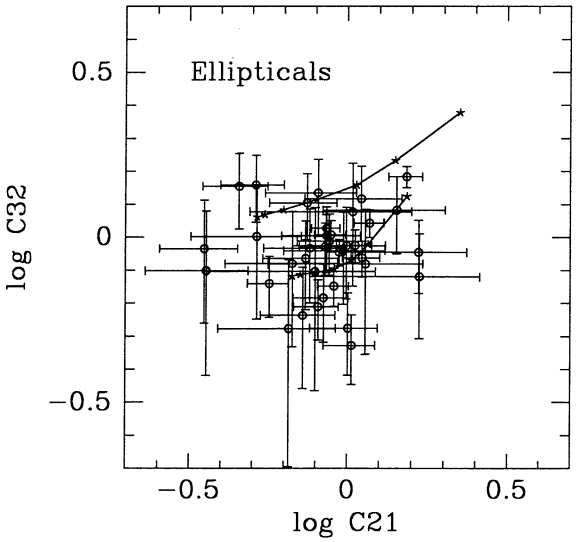

FIG. 3a

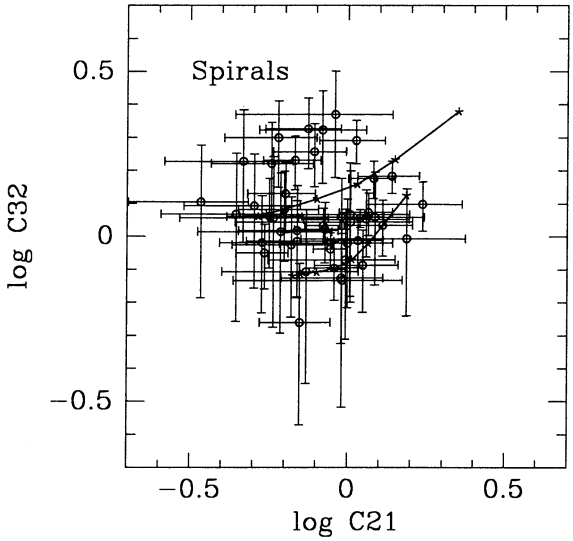

FIG. 3b

FIG. 3.—X-ray colors for (*a*) ellipticals and (*b*) spirals. The two lines are the same as in Fig. 1*b*.

colors of the two groups are well separated with a scatter comparable to the error of the mean in Figure 4. As discussed in § 2.3 these differences in colors are a convincing indication of differences in the average emission spectra.

Figure 3 suggests that at least in part the harder spectrum of spirals might be due to a group of galaxies with a very high value of C32. These galaxies are all Sb and later types (see below); however, within these morphological types a large spread of C32 is observed. This may suggest different emission components in spirals, which may dominate the emission of different galaxies. However, the uncertainties on each color determination are such that we cannot pursue this point further in this paper. Future X-ray observations should be aimed at these galaxies to explore this possibility.

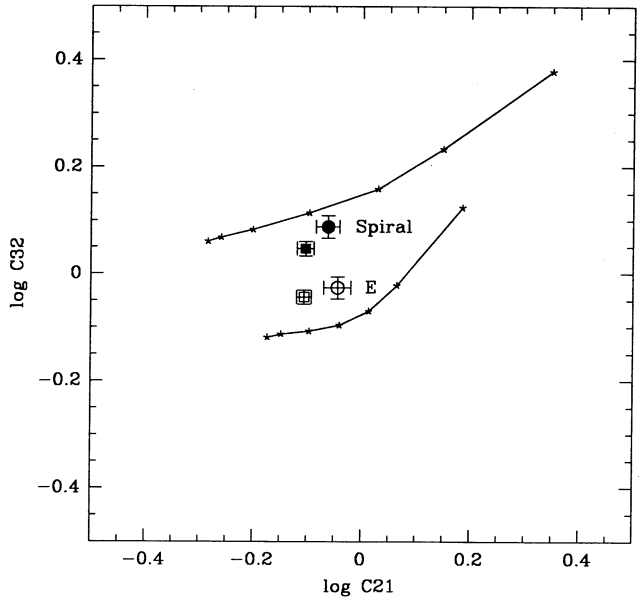

FIG. 4.—Means and errors for the colors of ellipticals (*open*) and spirals (*filled*) shown in Fig. 3. The squares denote X-ray colors weighted by the inverse square error of an individual estimate, while the circles are X-ray colors with an equal weight. The two lines are the same as in Fig. 1*b*.

In Figure 7 we plot the combined observed IPC spectra of elliptical and spiral galaxies (normalized at 2.4 keV). This figure shows clearly that the spectrum of spirals is significantly harder than that of ellipticals, in agreement with the distribution of colors. Figure 8 shows the confidence contours from the model fitting of the combined spectra of ellipticals and spirals. Ellipticals are well fitted with $kT = 1.4$–1.7 keV at the 90% confidence level. For spirals, the acceptable temperature is higher than 3 keV. This confirms that, on the average, spiral galaxies have higher emission temperature than elliptical galaxies. Notice that for the spirals we show two sets of contours: one from the fit to a Raymond model, and one from the fit to an exponential plus Gaunt (bremsstrahlung) model. Both give similar values for kT, but the Raymond model gives slightly lower values of N_H. As discussed in § 2.1, this is due to differences in the models. Given this "feature," and the similarity in the C21 colors, we conclude that on the average spirals do not appear to be more absorbed than ellipticals. This is surprising, since it is well known that spirals have larger amounts of cold interstellar matter than ellipticals. However, in Paper I we have shown that the spectral fits of some individual early-type galaxies reveal large N_H values, in excess of the line-of-sight hydrogen columns.

4.2. *Further Morphological Subdivisions*

As discussed above, there are definite spectral differences between elliptical and spiral galaxies. The next question that one may ask is: are there any differences in the spectral properties if we look at a finer subdivision of morphological types? To address this point we have first plotted the X-ray colors as a function of the morphological type (Fig. 9). We have used the parameter T from RC2 (de Vaucouleurs, de Vaucouleurs, & Corwin 1976, hereafter RC2) as an index of morphological type. No correlation between C21 and morphological type is seen, suggesting that on the average the X-ray spectra of late-type galaxies are not more absorbed at the low-energies than those of early-type galaxies. C32 instead is correlated with

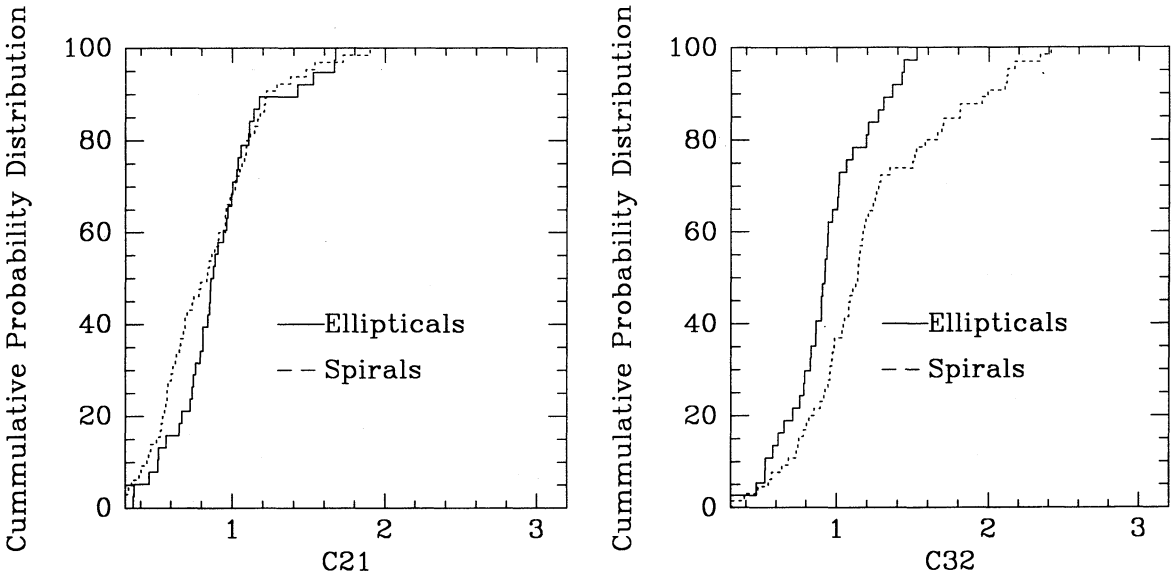

FIG. 5.—Cumulative probability distribution of C21 and C32 by Kolmogorov-Smirnov test

morphological type in the sense that later-type galaxies have harder X-ray spectra (larger kT). Confidence levels of independence are 0.7 and 0.0004 for the C21-T and C32-T relations, respectively, using the generalized Kendall's method (we used the software provided by E. D. Feigelson and T. Isobe). The best-fit regression lines of the C32-T relation are shown in Figure 9 and are given below:

$$\log (\mathrm{C32}) = 0.015 \times T + 0.009$$

$$T = 12.8 \times \log (\mathrm{C32}) + 0.39$$

To investigate further and to quantify these differences, we have then studied the average spectral properties of galaxies in different morphological subgroups: E ($T = -5$), E/S0 ($T = -3$), S0 ($T = -2$), Sa ($T = 0, 1, 2$), Sb ($T = 3, 4$), and Sc + Sd ($T > 4$). Figure 10 shows the combined observed spectra of different morphological subgroups. All these spectra are normalized at 2.4 keV. The spectra of E and E/S0 are similar; the S0 spectrum is slightly harder. For spiral galaxies, the spectra of later types (Sb and Scd) are similar, while the Sa spectrum is significantly softer, closer to the S0 spectrum. The average colors of these subgroups are plotted in a color-color plot in Figure 11. Sb and Sc are near the 5 keV line and the others are close together, slightly above the 1 keV line. We have fitted the combined spectra to the standard emission models, and we show the resulting confidence contours in

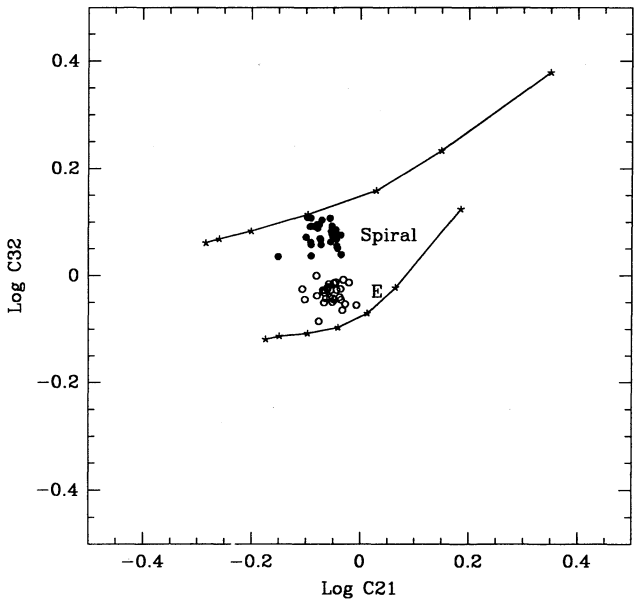

FIG. 6.—Means of X-ray colors for ellipticals (*filled circle*) and spirals (*open circle*) estimated by simulations (*see text*). The two lines are the same as in Fig. 1*b*.

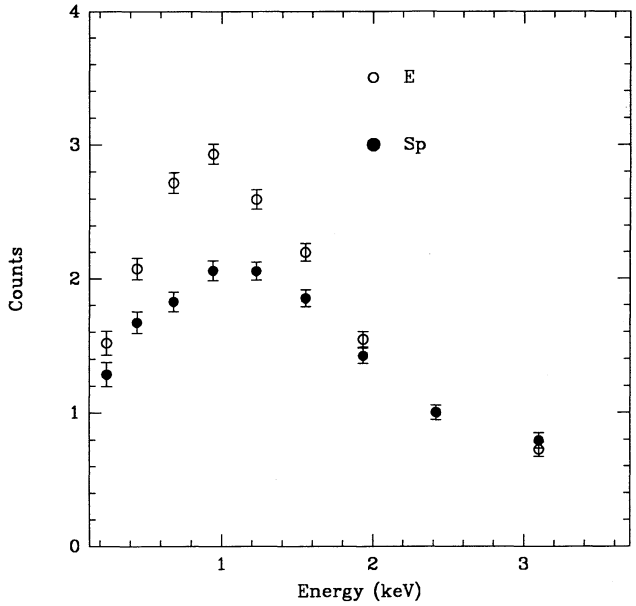

FIG. 7.—Combined observed distributions of spectral counts of ellipticals (*open circles*) and spirals (*filled circles*), normalized at 2.4 keV. The y-axis is in arbitrary units of log counts.

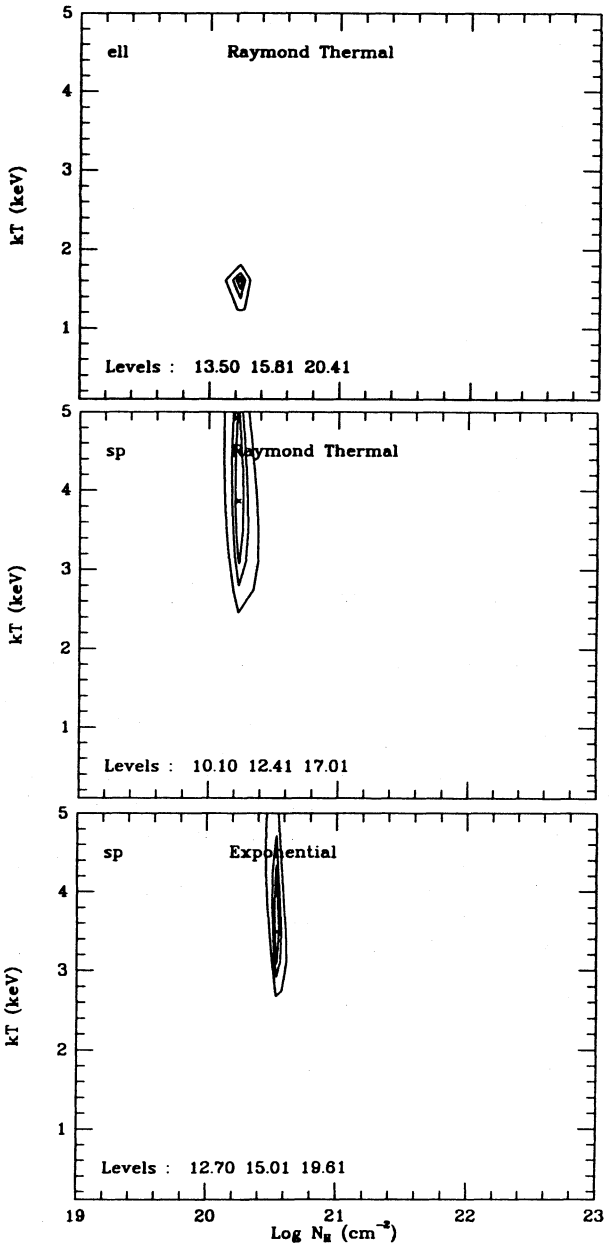

FIG. 8.—68%, 90%, and 99% confidence χ^2 contours with kT and N_H grids for elliptical and spiral galaxies. For spirals we show the results of the fit to a Raymond thermal spectrum and to a bremssthralung spectrum (exponential + Gaunt). These give the same results for kT, but slightly different N_H (*see text*).

Figure 12. We summarize in Table 1 the range of the parameters at the 90% confidence level. From Table 1 and Figure 12 it is interesting to notice that the allowed kT range of Sa (and to a lesser extent S0) galaxies stretches to include values allowed by the fits to both E and later-type S galaxies. We ask the question: is this an indication of intermediate spectral properties of these intermediate morphological types, or just a quirk of statistics?

To answer the above question, we have performed a simulation with two input spectra: the combined spectrum of elliptical galaxies ($T = -5$), and that of Sc + Sd ($T > 4$). We have used these spectra (with estimated errors) as seeds for a ran-

TABLE 1

X-RAY SPECTRAL PROPERTIES OF DIFFERENT MORPHOLOGICAL TYPES[a]

Type	Number[b]	kT (keV)	N_H (cm^{-2})	χ^2 (7)
		Raymond		
E	18	1.2 (1.2–1.7)	1.7 (0.9–2.6) × 10^{20}	7.3
E/S0	7	1.2 (1.2–1.7)	1.7 (1.2–4.4) × 10^{20}	11.3
S0	12	1.6 (1.5–2.2)	1.7 (1.1–2.1) × 10^{20}	4.8
E + S0	37	1.6 (1.4–1.7)	1.7 (1.5–1.8) × 10^{20}	11.2
		Bremsstrahlung		
Sa	9	1.6 (1.2–3.3)	7.1 (3.2–10) × 10^{20}	10.7
Sb	15	4.3 (2.8–)	3.5 (1.6–4.4) × 10^{20}	7.2
Sc + Sd	22	4.6 (3.1–)	3.5 (2.5–4.6) × 10^{20}	6.1
Sa + Sb + Sc	46	3.5 (2.9–4.7)	3.5 (3.1–3.9) × 10^{20}	10.4

[a] Given are the best-fit values of kT and N_H and the 90% ranges (in parentheses).

[b] Number of galaxies in each composite spectrum.

domization program, creating 100 randomly generated spectra from each. Because the errors on the simulated spectrum will be of a similar order of magnitude as that of the input spectrum, we did not simulate the errors and used those of the input spectrum. We then performed a spectral analysis on each of these spectra and generated confidence contours. We find that we obtain confidence contours comparable to those of Sa galaxies only 3% of the time from the hard (late-type S) spectrum and never from the soft (E) spectrum. This shows that it is very unlikely that Sa-type confidence contours would arise from a "pure" E spectrum, and fairly unlikely that they would arise from a hard late-type spectrum. It suggests that Sa galaxies have more than one spectral emission component. To investigate this further we have obtained spectra by mixing the two original input spectra in varying proportions. Confidence contours similar to those of the Sa fits are obtained by mixing E and Scd spectra in approximately equal amounts (ratios of 4 to 6 and 6 to 4 are not excluded).

We conclude that the spectra of Sa galaxies are intermediate between those of elliptical and spirals. This result suggests that these galaxies contain hot gaseous emission as well as emission from accreting stellar binaries.

About 40% of the composite Sa spectrum is due to NGC 4579, which is fitted with relatively high kT values (Paper I). This galaxy has a LINER nucleus (Willner et al. 1985). To make sure that our results are not biased by the presence of this source, we repeated the analysis without NGC 4579, and found almost identical results as in Figure 12. We also constructed mean colors, as in the previous section, equally weighting each individual galaxy. These colors are consistent with the composite colors of Figure 11, within the errors.

5. SPECTRAL PROPERTIES AND L_X/L_B OF ELLIPTICAL GALAXIES

5.1. *Hot Interstellar Medium and Binary X-Ray Sources*

The origin of the X-ray emission of X-ray faint elliptical galaxies has been a matter of debate. Forman et al. (1985; see also Jones 1987) conclude that all of the emission of early-type galaxies with absolute blue magnitude $M_B \leq -19$ is due to hot gaseous halos. Trinchieri & Fabbiano (1985), Canizares et al. (1987), and Fabbiano et al. (1989) argue instead that the data require the presence of a gaseous component only in the more

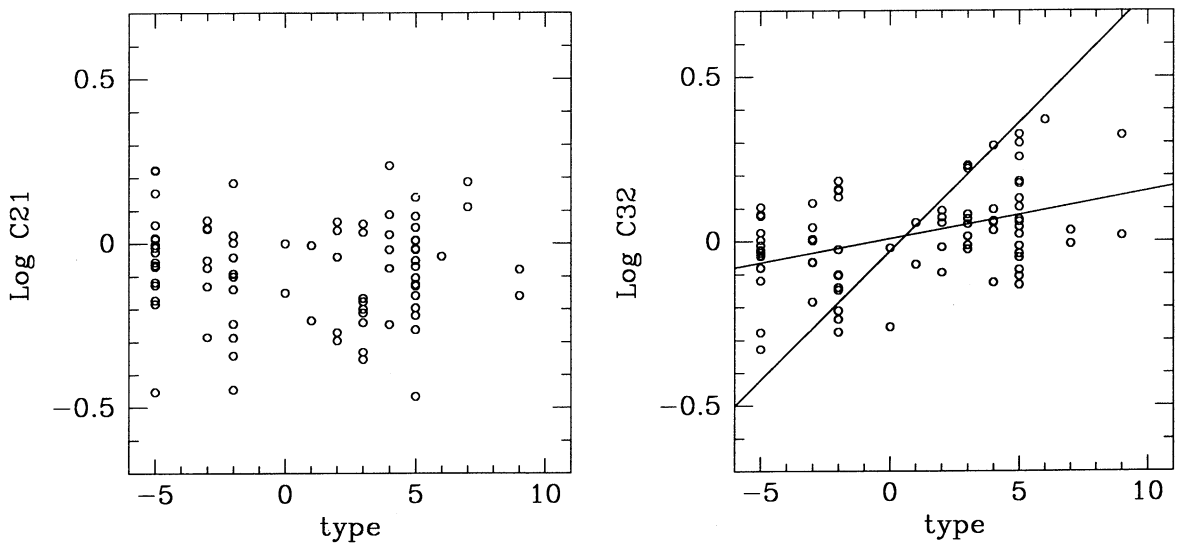

FIG. 9.—X-ray colors vs. morphological type. We use the parameter T from RC2 to characterize the morphological type. Only C32 appears to be correlated with T. The two least-squares-fit lines (log C32 vs. T and T vs. log C32) are drawn.

X-ray–luminous galaxies, while the emission of galaxies less luminous than $10^{40.5-41}$ ergs s^{-1} (these galaxies can be optically very bright, with $M_B \sim -22$) can be easily explained with a population of accreting low-mass binary sources. Since in spiral galaxies, where the X-ray emission is likely to be dominated by stellar sources, the X-ray and optical emission are linearly correlated, Fabbiano et al (1989) suggest the use of the X-ray to optical luminosity ratio as a measure of excess X-ray emission, which is presumably due to a gaseous halo.

To explore this issue, we have divided elliptical (E, E/S0, and S0) galaxies into four subgroups according to their L_X/L_B ratio (L_X in ergs s^{-1} from Fabbiano et al. 1992 and L_B in $L_\odot$ derived using the magnitudes and distances tabulated in Fabbiano et al. 1992 following the definition given in Canizares et al. 1987), putting roughly the same number of galaxies in each group. Table 2 lists L_X/L_B in the above units for groups 1 to 4 and the galaxies belonging to each group. The combined spectra are shown in Figure 13 and are compared to the combined spectra of all spiral and elliptical galaxies discussed in § 4.1. We have excluded NGC 507 and NGC 3607 (see below).

Except for the lowest L_X/L_B group (see § 5.2), as L_x/L_B decreases, the spectra become harder, resembling those of spirals. This trend is also suggested by the color-color plot (Fig. 14). The C32 indices for groups 2 and 4 differ at the 2.7 σ level. The 90% confidence regions for groups 2 and 4 obtained from model fitting of the composite spectra are also well disjoint (Fig. 15). The spectral contours suggest a probability of less than 10^{-3} that the emission temperatures are the same for groups 2 and 4. Moreover, our simulation of § 4.2 shows that it is very unlikely that a group 4 soft spectrum could give rise to confidence contours shaped like those of group 2. This result needs to be confirmed with higher statistical significance such

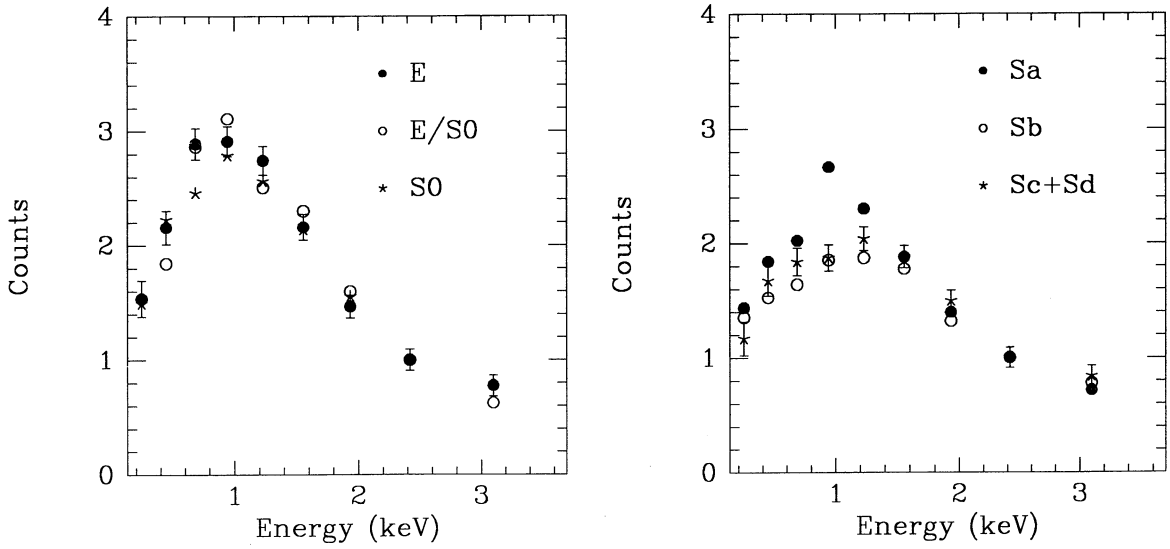

FIG. 10.—Combined spectra of different morphological types of galaxies (normalized at 2.4 keV). Representative error bars are shown. The y-axis is in units of counts.

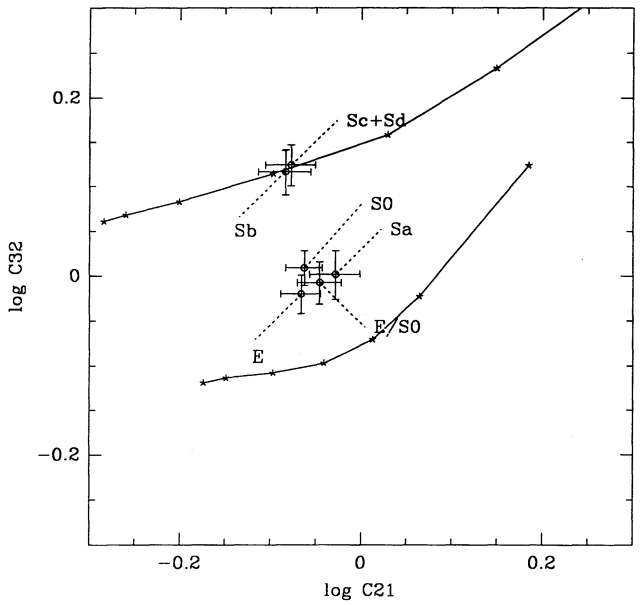

FIG. 11.—Color-color plot for the combined spectra shown in Fig. 10. The two lines are the same as in Fig. 1*b*.

as may be achieved with long *ROSAT* observations of these galaxies. However, as it stands, it is in the sense we would expect if a low-mass binary component is more important in X-ray–faint ellipticals and gaseous emission is dominant in X-ray–luminous ellipticals.

Because S0 galaxies are intermediate in spectral properties between spirals and ellipticals and in general less bright than ellipticals, they might affect the above results. Therefore we repeated the above analysis excluding S0 galaxies. We found the same trend that emission temperature decreases as L_X/L_B increases. We also excluded the highest signal-to-noise source in each group to check if the very bright object dominates the results. We again obtained the same trend.

That the results are not dominated by a few strange objects in each subgroup is also shown by Figure 16, where the objects in each subgroup are plotted singly in color-color plots. This figure shows that the distributions of individual points are reasonably delimited, with few exceptions. These include NGC 507 and NGC 4203 in the highest L_X/L_B group (group 4), and NGC 3607 and NGC 4552 in the group with the harder spectra (group 2). Both NGC 507 and NGC 4203 have higher kT than the other galaxies in group 4. NGC 507 is very X-ray luminous, more in the range of groups and clusters than in that of isolated galaxies, and its higher X-ray temperature is similar to those observed in groups, pointing to a deeper potential well (see Paper I; Kim, Fabbiano, & Eskridge 1992). As mentioned above, this galaxy was excluded from our analysis. Retaining it would result in a considerable hardening of the Group 4 spectrum, because NGC 507 is detected at a very high signal-to-noise ratio.

NGC 4203 does not have an extremely high L_X/L_B, so the discrepancy is not easily understandable. NGC 4203 does have H I gas in a shell structure (van Driel et al. 1988). Interestingly, the spatial distribution of X-ray emission and H I gas appear related when the X-ray image in Fabbiano et al. (1992) and Figure 5 in van Driel et al. (1988) are compared. The X-ray emission is sharply bounded toward P.A. = −135° to 0° where the H I shell is present, while the elongation of X-ray surface brightness distribution is toward P.A. = 90°–180° where the least amount of H I gas is present. However, it is not obvious, with the noisy IPC spectral data, that the region at P.A. = 90°–180° shows less absorption than the rest of the galaxy.

NGC 3607 and NGC 4552 have colors too soft for their X-ray to optical luminosity ratios. However, the emission of NGC 3607 may be contaminated by the X-ray emission of nearby strong sources (see Fabbiano et al. 1992). NGC 3607 has the lowest L_X/L_B in group 2 and perhaps should be grouped with group 1. For these reasons we have excluded this galaxy when deriving the composite group 2 spectrum and colors. The X-ray image of NGC 4552 is consistent with a pointlike distribution of photons (Fabbiano et al. 1992). It is therefore possible that the emission contains a nuclear component. However, high-resolution X-ray observations will be needed to address this point.

TABLE 2

E AND S0 GALAXIES RANKED BY L_X/L_B

Galaxy (NGC)	log (L_X/L_B)
Group 1	
4526	29.32
4365	29.61
4697	29.68
4382	29.71
5838	29.72
1316	29.92
Group 2	
3607[a]	30.11
4168	30.12
4552	30.19
IC 1459	30.19
4374	30.20
1052	30.22
1332	30.23
3923	30.24
Group 3	
5077	30.26
3078	30.29
1395	30.41
1407	30.41
5353	30.47
4649	30.49
7626	30.51
IC 4296	30.57
720	30.58
4291	30.70
4472	30.73
Group 4	
1404	30.83
6876	30.84
7619	30.93
4203	31.03
5846	31.05
4636	31.13
2563	31.13
4406	31.19
4756	31.29
499	31.42
507[a]	31.56
5044	32.13

[a] Excluded from composite spectrum (see text).

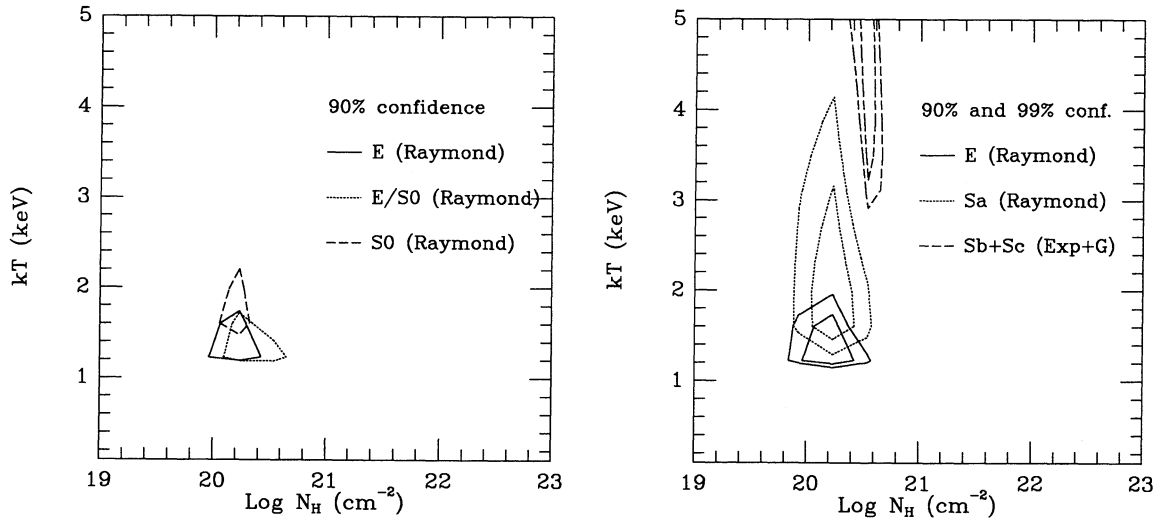

FIG. 12.—*Left*: 90% confidence regions for a χ^2 fit to a Raymond emission model of the composite spectra of E, E/S0, and S0 galaxies; *Right*: 90% and 99% confidence regions for E, Sa, Sb, and Sc galaxies. The results for Sb and Sc are the same, and we show only the Sb contours. The shift in N_H is due to the different models used for the fit (see § 4.1).

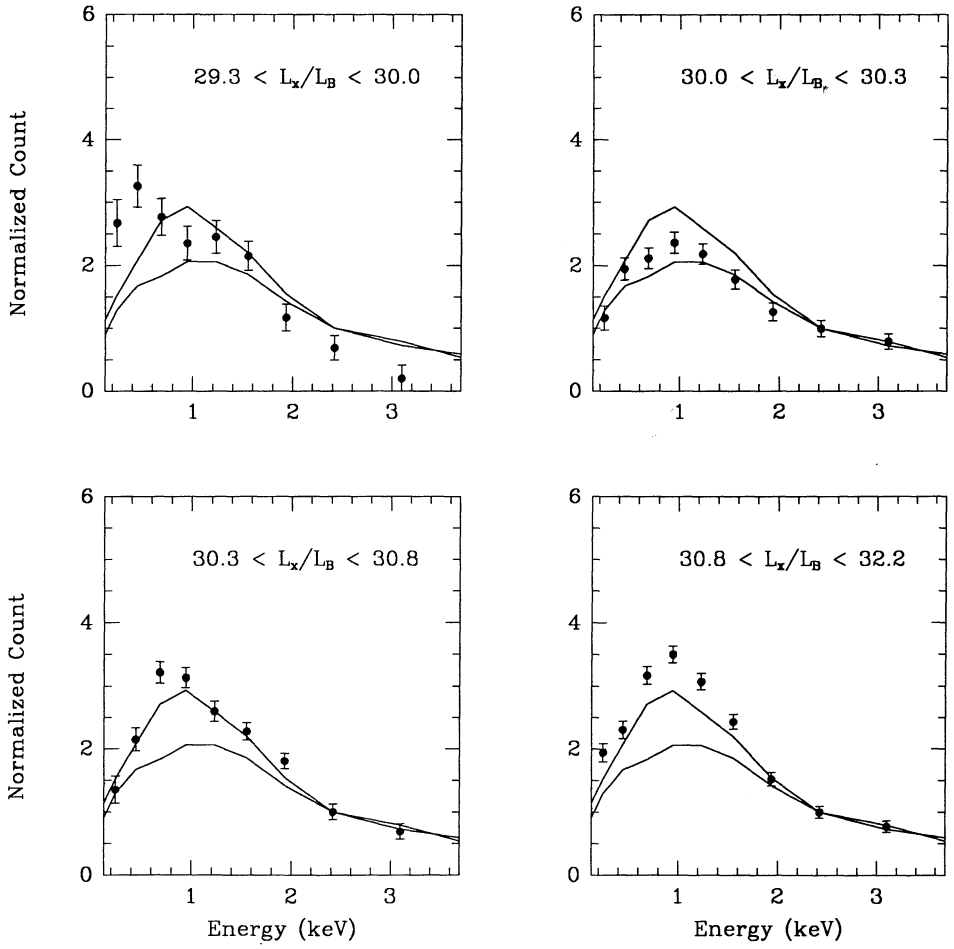

FIG. 13.—Combined spectra of early-type galaxies grouped by L_X/L_B. The two lines represent the composite spectra of ellipticals (*upper*) and spirals (*lower*), shown in Fig. 6. The combined spectra of the four L_X/L_B groups have been arbitrarily renormalized to match these curves. The *y*-axis is in units of counts.

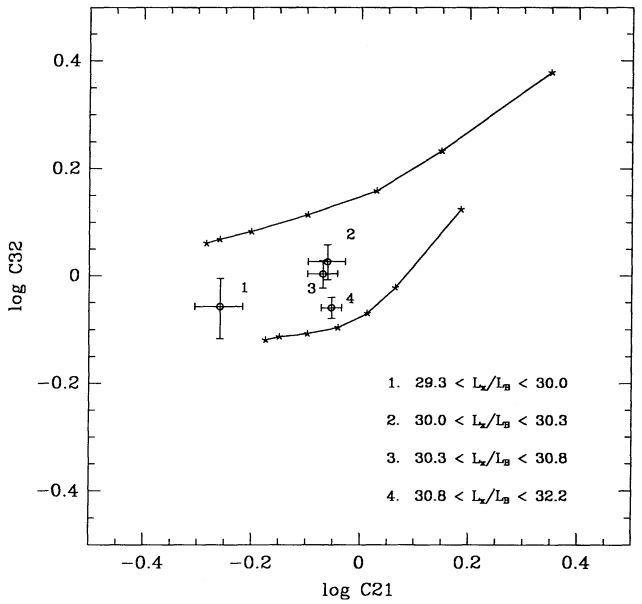

FIG. 14.—X-ray color-color plot of early-type galaxies grouped by L_X/L_B. The two lines are the same as in Fig. 1.

5.2. *The Very Soft Component of X-Ray Faint Galaxies*

The group with the lowest L_X/L_B (group 1) has a rising spectrum at the low energies. The X-ray colors and the spectral fit to the composite spectrum give a range of N_H lower than typical Galactic values. These values are different from those, for example, of group 4 at a high confidence level: the C21 colors of groups 1 and 4 differ at greater than 5 σ level, and the 99% confidence contours from the spectral fits of the composite spectra barely touch ($P \sim 10^{-4}$). The N_H values of group 1 are unphysical because the X-ray emission will have to experience at least line-of-sight absorption, and suggest that a simple cutoff spectrum is not a good model for the distribution of the IPC counts. They suggest that a very soft spectral component may be present in addition to a harder (e.g., group 2) spectrum (see Wilkes & Elvis 1987 for a detailed discussion of a similar effect in QSOs). This component will have the effect of mimicking a smaller low-energy cutoff. Since group 1 comprises the galaxies with the lowest signal-to-noise ratio, we worried that this result may be caused by some flaw in our data analysis. To check this point, we have taken galaxies from the other groups, and we have artificially made spectra with similar signal-to-noise ratios to that of group 1 by dividing the images in four azimuthal sectors centered on the source centroids and then combining the spectra of each quadrant. The signal-to-noise

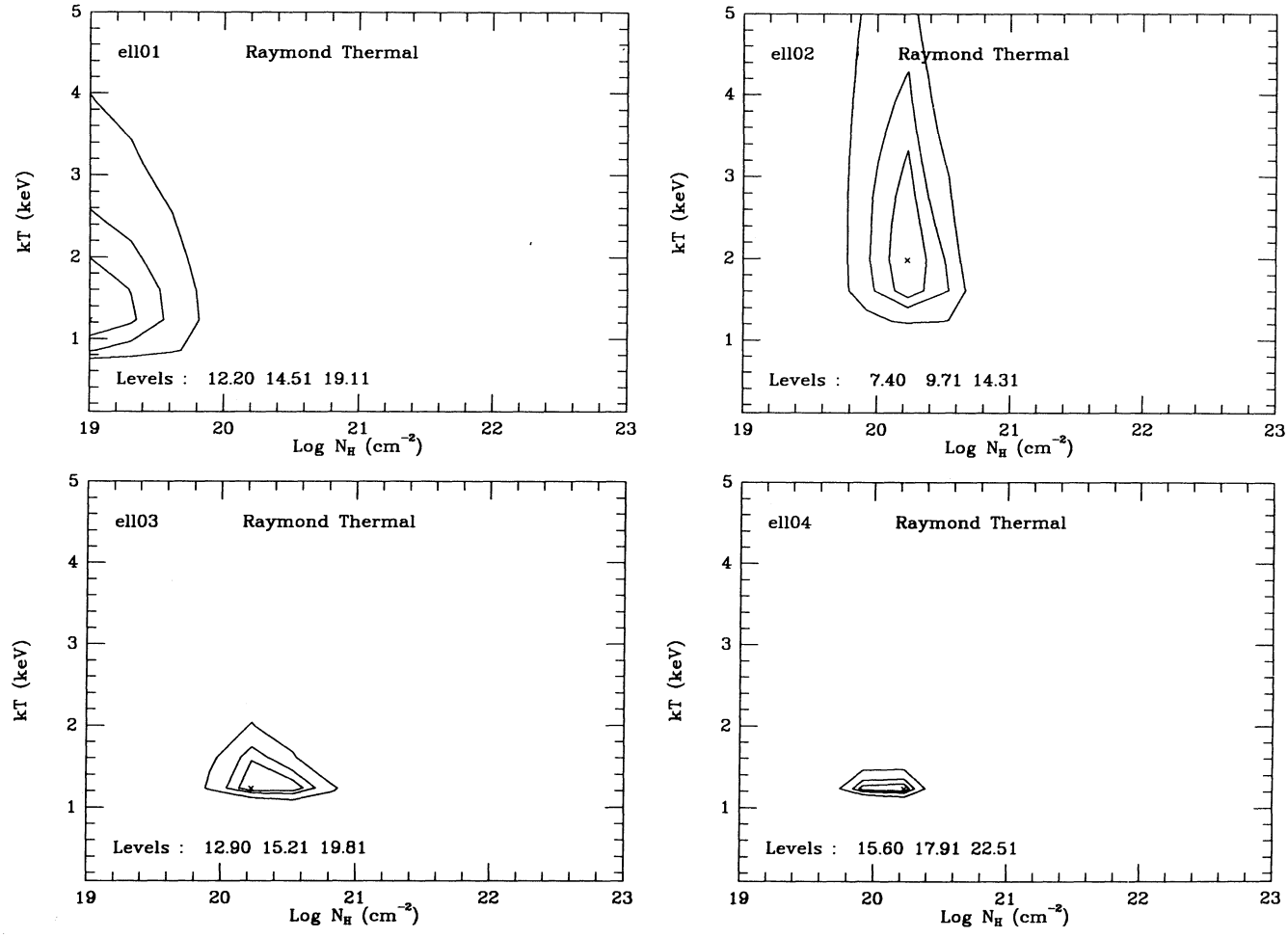

FIG. 15.—68%, 90%, and 99% confidence contours for early-type galaxies grouped by L_X/L_B

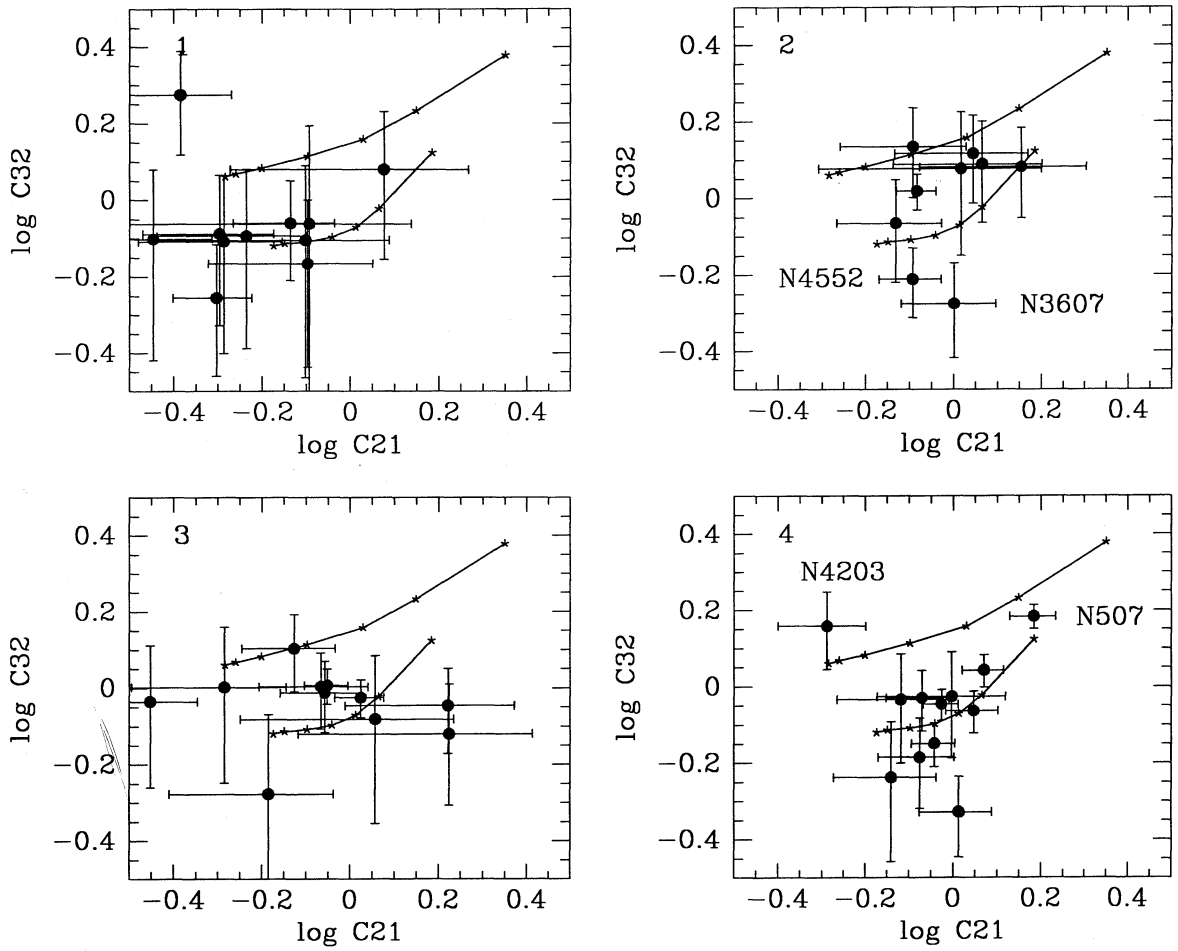

FIG. 16.—X-ray colors of individual galaxy in four subgroups divided according to L_X/L_B

ratio in group 1 is 22 and those of each quadrant range 16–20, 22–32, and 25–30 in groups 2, 3, and 4, respectively. In group 4, background counts were estimated by using quadrants in order to lower the signal-to-noise ratio, while in groups 2 and 3, we used an annulus surrounding the source (see Paper I). The X-ray colors of four subsections in groups 2, 3, and 4 are shown in Figure 17. This figure demonstrates how the colors for each subgroup are spread around the composite colors of Figure 14, and cannot reproduce the composite colors of group 1. It is unlikely, therefore, that the very soft excess is due to a low signal-to-noise ratio.

To have an estimate of the luminosities of these very soft components, we have assumed that the composite spectrum of group 1 is due to a hard group 2–like spectrum, which we have modeled with a 5 keV thermal emission, plus a second thermal component. We have allowed the temperature of this second component and the intensities of the two components to vary as free parameters, and fixed log $(N_H) = 20.5$. The results of a χ^2 fit are given in Figure 18. The data are best fitted with a very soft emission of 0.2 keV with $\chi^2 = 10.2$ for 6 degrees of freedom ($kT = 0.16$–0.22 at the 90% confidence level). The luminosity of this soft excess emission is approximately half ($\sim 10^{40}$ ergs s^{-1}) of the total emission in the 0.2–3.5 keV range.

Are our results consistent with this component always being there, or is it there only in group 1? If this soft X-ray lumi-

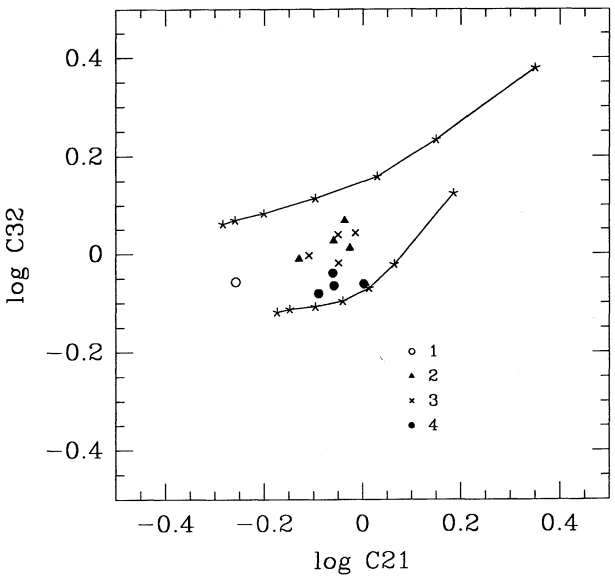

FIG. 17.—Results of a simulation done to demonstrate that the very soft colors of group 1 (the lowest L_X/L_B group) are not due to the poorer signal-to-noise ratio of these detections (*see text*). We plot X-ray colors of subsections of each group in Fig. 14. Each group is divided spatially into four subsections and colors are estimated in each subsection.

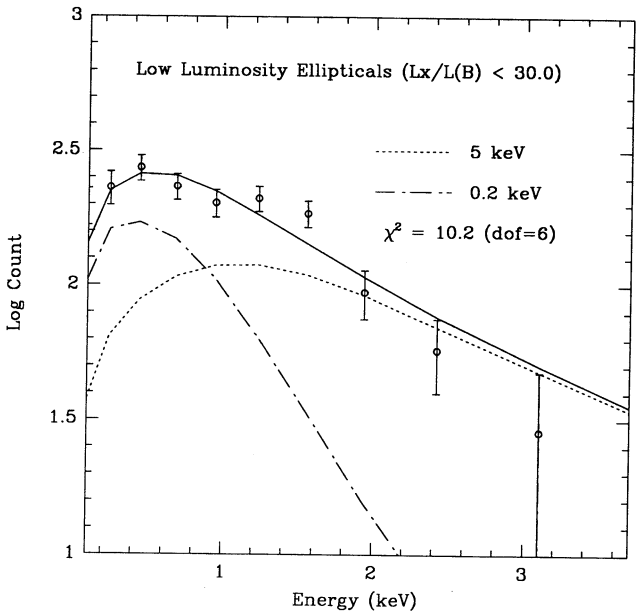

FIG. 18.—Two-component fit to the spectrum of the lowest L_X/L_B group. The solid line represents the two-component spectrum, and the dot-dashed and the dotted lines represent the very soft and the 5 keV components, respectively.

nosity is proportional to the blue luminosity, it would be approximately one-sixth of the total X-ray luminosity for group 2, one-eighteenth for group 3, and one seventy-sixth for group 4. It would not be possible to detect this soft component in groups 3 and 4. Even in group 2, with the IPC data we would not detect the presence of the soft component. This is shown in Figure 19, where the group 2 spectrum is compared with a mixed one ($\frac{5}{6}$ of 5 keV spectrum + $\frac{1}{6}$ of 0.2 keV spectrum). With the available data, it remains possible that this soft component is present in all early-type galaxies.

What produces this very soft X-ray emission? One possibility is gaseous emission with lower temperature. The $L_X \sim 10^{40}$ ergs s^{-1} that we estimate for this component is well in excess of that predicted by wind models (e.g., D'Ercole et al. 1989; David, Forman, & Jones 1991; Ciotti et al. 1991). Therefore if this emission is of gaseous origin, it may suggest that these galaxies do not heat their ISM to X-ray temperatures. Perhaps they have a very low supernova rate. If instead, as discussed above, the very soft component is present in all early-type galaxies, but visible only in the X-ray–faintest ones, we may be detecting emission from the stellar population. Possibilities include the integrated contribution of M stars (see, e.g., the discussion in Feigelson et al. 1981), or ultrasoft binaries, similar to those detected with *ROSAT* in the LMC (Hasinger 1991). In the case of NGC 1316 (Fornax A) it is also possible that we are detecting a soft nuclear emission component. It is known that some AGNs have very soft components (e.g., Wilkes & Elvis 1987; Fabbiano 1988a; Kruper, Urry, & Canizares 1990; Paper I).

6. SPIRAL GALAXIES

6.1. *Very Soft Component*

In general, the average X-ray spectrum of spiral galaxies is hard (see § 4.1). However, there are galaxies in our sample which seem to have additional very soft X-ray components. Figure 20 shows that the X-ray colors of some galaxies imply absorption columns below the line of sight N_H, which is usually $\geq 10^{20}$ cm^{-2} (see Fabbiano et al. 1992). As discussed in § 5.2, these N_H values are unphysical because the X-ray emission will have to experience line-of-sight absorption and most likely also absorption within the parent galaxy. This effect suggests that a very soft component may be present. To explore this point, we have chosen the 10 galaxies with C21 < 0.6 of Paper I, which fit our selection criteria (see § 3). These are indicated by filled dots and a triangle (for NGC 253) in Figure 20 and are

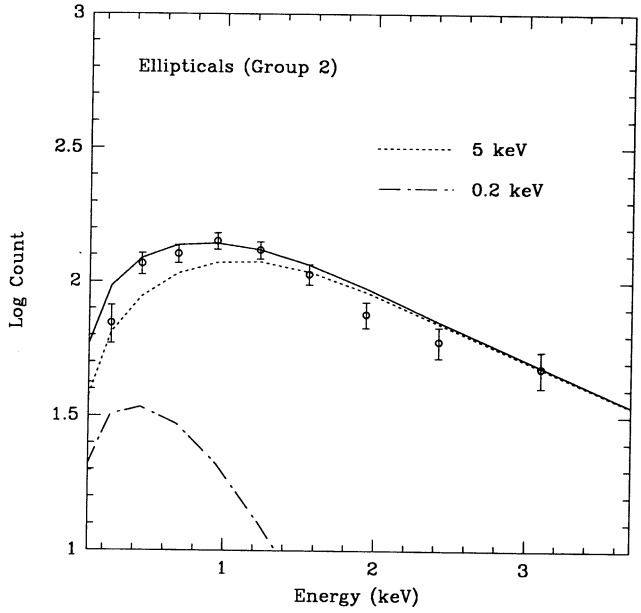

FIG. 19.—Two-component fit to the spectrum of group 2. The group 2 spectrum is compared with a mixed spectrum ($\frac{5}{6}$ of 5 keV spectrum + $\frac{1}{6}$ of 0.2 keV spectrum).

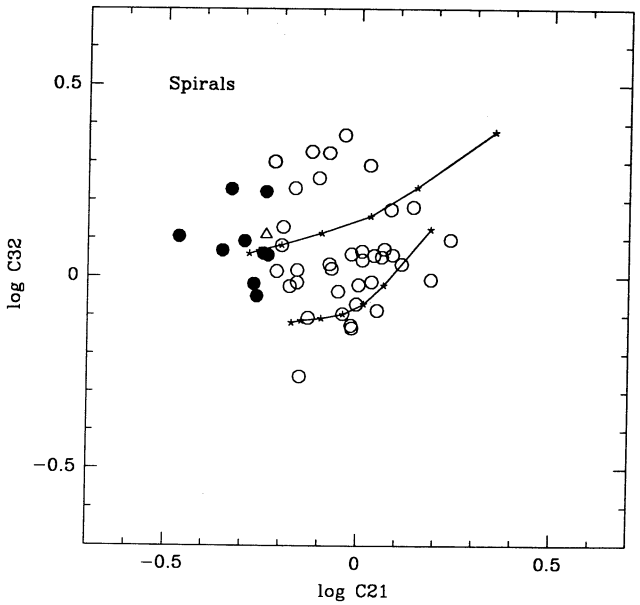

FIG. 20.—Color-color plot of spiral galaxies. Filled dots indicates galaxies with very soft colors; the triangle indicates NGC 253. The two lines are the same as in Fig. 1*b*.

TABLE 3

SPIRALS WITH SOFT EXCESSES (C21 < 0.6)

Galaxy (NGC)	Type (T)	$N_H^{\text{line-of-sight}}$ (cm^{-2})
247	5	1.5×10^{20}
253	5	1.3×10^{20}
1398	2	9.7×10^{19}
1672	3	2.2×10^{20}
2841	3	1.4×10^{20}
3081	1	4.5×10^{20}
4303	5	1.7×10^{20}
4450	2	2.4×10^{20}
4501	4	2.5×10^{20}
4826[a]	2	2.6×10^{20}
6872	3	5.2×10^{20}

[a] This galaxy is not part of the sample (see § 3).

listed in Table 3. In Table 3 we also give the morphological parameter T from RC2 for each galaxy; the wide range of T shows that the presence of the soft component is not linked to the galaxy morphology. The presence of a soft component is evident when looking at the composite gain-corrected distribution of spectral counts of these galaxies, in comparison with the composite spectrum of the entire spiral sample (Fig. 21). We fitted the spectrum to a two-component model (soft component + 5 keV component), treating the emission temperature of the soft component and the intensities of the two components as free parameters. A mixture of 30% of 0.07 (0.06–0.08 at the 90% confidence level) keV component plus 70% of 5 keV component with fixed log (N_H) = 20.5 gives the best fit with $\chi^2 = 13$ for 6 degrees of freedom (Fig. 22).

NGC 253 (marked by a triangle in Fig. 20), which has direct imaging evidence for a gaseous plume and possibly diffuse large-scale emission (Fabbiano & Trinchieri 1984; Fabbiano 1988b), belongs to this group. Although we cannot determine the nature of this soft emission with the *Einstein* data alone, one obvious possibility is hot gaseous emission as in NGC 253.

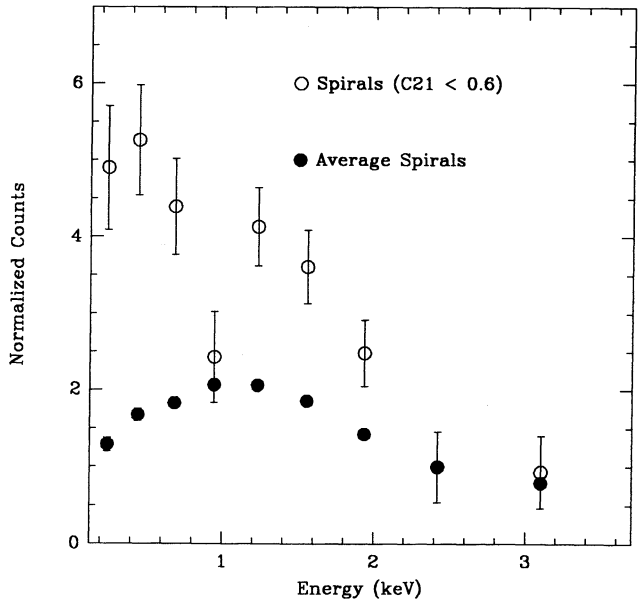

FIG. 21.—Composite spectrum of soft spirals (*open circles*) normalized at 2.4 keV, compared with the average spectrum of spirals (*filled circles*). The y-axis is in units of counts.

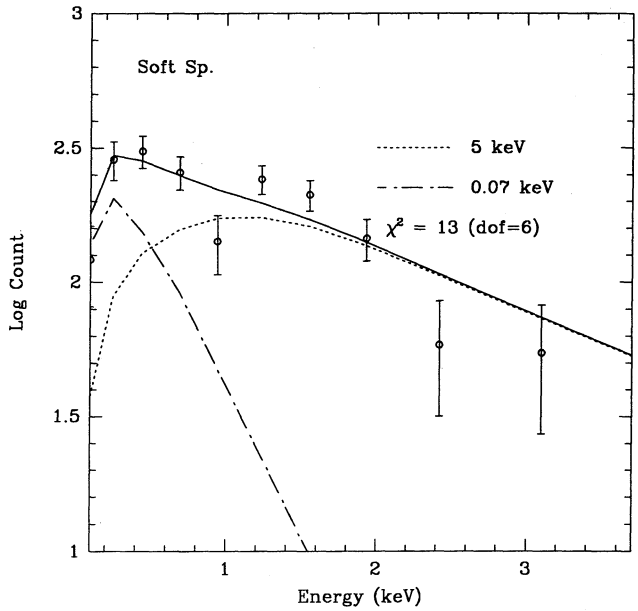

FIG. 22.—Two-component fit to the spectrum in Fig. 21

One of the standing puzzles in our understanding of the ISM of spiral galaxies is the lack of a hot X-ray–emitting phase (see Fabbiano 1989 and references therein). Given the typical supernova energy input in a spiral galaxy, this component of the ISM could emit up to 10^{42} ergs s^{-1}. This is well above the average L_X of spirals detected with *Einstein* (e.g., Fabbiano et al. 1992). Moreover, the X-ray emission of spirals appears to be dominated by hard X-ray sources, such as accretion binaries (see Fabbiano 1989; Paper I, § 4). As a consequence of this lack of detection of an X-ray–emitting ISM, it has been suggested that the hot ISM is probably emitting in a softer band, below the *Einstein* spectral limit (e.g., Cox 1983). The very soft component that we have discovered in spiral galaxies might be giving us a first glimpse at this hot ISM. The alternate explanation of a population of soft discrete sources, as discussed in § 5.2, is also possible. *ROSAT* observations would be useful to identify the properties of this soft excess.

6.2. *Inclination*

We looked for an inclination effect on the X-ray spectra. It could be expected that stronger absorption in edge-on spiral galaxies would cause harder X-ray spectra. This effect would result in larger C21 in edge-on than in face-on spiral galaxies. However, when we plot C21 versus the ratio of major and minor axes, taken from RC2, we find no hint of correlation in our spiral sample (not shown). The generalized Kendall's method gives a probability of correlation arising by chance of 0.96. Possibly our sensitivity to determining the H I column density is not good enough. Quantitatively, the acceptable range of slope (0.01 ± 0.24) in the relation of log (C21) and log (major-axis/minor-axis) still allows almost an order of magnitude change in H I column density from 10^{20} to 10^{21} cm^{-2} between edge-on and face-on galaxies.

7. CONCLUSIONS

We summarize our main results as follows:

1. On the average, spirals ($kT > 3$ keV) have higher emission temperature than ellipticals ($kT = 1$–2 keV). This supports the

idea that in elliptical galaxies hot gaseous halos dominate X-ray emission, while in spiral galaxies accreting binaries are a major X-ray source.

2. Sa galaxies are intermediate in X-ray spectral properties between ellipticals and later-type spirals, indicating that they have stellar emission as well as hot gaseous emission.

3. If we use the L_X/L_B ratio as a discriminator, we find that X-ray–faint ellipticals have higher emission temperature than X-ray–bright ellipticals. This (in addition to the L_X/L_B diagram) suggests that X-ray–faint ellipticals do not retain their hot ISM.

4. Early-type galaxies in the lowest L_X/L_B group have a *very soft* X-ray excess which amounts to about half the total X-ray emission. The nature of this component is not clear: it could be due either to a cooler ISM, or to the integrated emission of soft stellar sources.

5. There is no significant difference in absorption column density between ellipticals and spirals. We do not find an increase in column density of edge-on spiral galaxies, compared with the face-on spirals.

6. Although in general the X-ray spectrum of spirals is hard, there are several galaxies with unusually soft spectra. This may indicate that some spirals contain hot gaseous halos or outflows as in NGC 253.

These results show the potential of X-ray spectral studies for investigating the nature of the X-ray emission of different types of galaxies. Future X-ray observations, such as may be obtained with *ROSAT*, will be required to quantify these differences at a high statistical confidence.

We thank Saku Vrtilek for comments on the manuscript, and Alvio Renzini, Annibale D'Ercole, Luca Ciotti, and Silvia Pellegrini for discussions on the possible nature of the emission components of elliptical galaxies. This work was supported by NASA grant NAG 5-1202, NASA contract NAS 8-30751, and Smithsonian Institution Scholarly Studies grant S910. G. T. acknowledges financial support by the Italian ASI. D. W. K. acknowledges support by the 1991 Research Program of Chungnam National University.

REFERENCES

Canizares, C. R., Fabbiano, G., & Trinchieri, G. 1987, ApJ, 312, 503
Ciotti, L., D'Ercole, A., Pellegrini, S., & Renzini, A. 1991, ApJ, 376, 380
Cox, D. P. 1983, in IAU Symp. 101, Supernova Remnants and their X-Ray Emission, ed. J. Danziger & P. Gorenstein (Dordrecht: Reidel), 385
David, L. P., Forman, W., & Jones, C. 1991, ApJ, 369, 121
D'Ercole, A., Renzini, A., Ciotti, L., & Pellegrini, S. 1989, ApJ, 341, L9
de Vaucouleurs, G., de Vaucouleurs, A., & Corwin, H. 1976, Second Reference Catalogue of Bright Galaxies (Austin: Univ. of Texas) (RC2)
Fabbiano, G. 1988a, ApJ, 325, 544
———. 1988b, ApJ, 330, 672
———. 1989, ARA&A, 27, 87
Fabbiano, G., Feigelson, E., & Zamorani, G. 1982, ApJ, 256, 397
Fabbiano, G., Gioia, I. M., & Trinchieri, G. 1989, ApJ, 347, 127
Fabbiano, G., Heckman, T., & Keel, W. C. 1990, ApJ, 355, 442
Fabbiano, G., Kim, D.-W., & Trinchieri, G. 1992, ApJS, 80, 531
Fabbiano, G., & Trinchieri, G. 1984, ApJ, 268, 491
———. 1985, ApJ, 296, 430
———. 1987, ApJ, 315, 46
Fabbiano, G., Trinchieri, G., & Van Speybroeck, L. S. 1987, ApJ, 316, 127
Fabian, A. C. 1981, The Structure and Evolution of Normal Galaxies, ed. S. M. Lynden-Bell (Cambridge: Cambridge Univ. Press), 181
Feigelson, E. D., Schreier, E. J., Delvaille, J. P., Giacconi, R., Grindlay, J. E., & Lightman, A. P. 1981, ApJ, 251, 31
Forman, W., Jones, C., & Tucker, W. 1985, ApJ, 293, 102
Giacconi, R., et al. 1979, ApJ, 230, 540
Harnden, F. R., Jr., Fabricant, D., Harris, D., & Schwartz, J. 1984, Smithsonian Astrophys. Obs. Spec. Rep., No. 393
Harris, D. H. 1984, Einstein Observatory Revised User Manual, SAO internal report
Hasinger, G. 1991, talk given at Nagoya conference
Helfand, D. J. 1984, PASP, 96, 913
Jones, C. 1987, Nearly Normal Galaxies, ed. S. M. Faber (New York: Springer), 109
Kim, D.-W., Fabbiano, G., & Eskridge, P. B. 1992, in preparation
Kim, D.-W., Fabbiano, G., & Trinchieri, G. 1992, ApJS, 80, 645 (Paper I)
Kruper, J. S., Urry, C. M., & Canizares, C. R. 1990, ApJS, 74, 347
Stewart, G. C., Fabian, A. C., Terlevich, R. J., & Hazard, C. 1982, MNRAS, 200, 61
Trinchieri, G., & Fabbiano, G. 1985, ApJ, 296, 447
———. 1991, ApJ, 382, 82
Trinchieri, G., Fabbiano, G., & Peres, G. 1988, ApJ, 325, 531
Trinchieri, G., Fabbiano, G., & Romaine, S. 1990, ApJ, 356, 110
van Driel, W., van Woerden, H., Gallagher, J. S., & Schwarz, U. J. 1988, A&A, 191, 201
Watson, M. G., Stanger, V., & Griffiths, R. E. 1984, ApJ, 286, 144
Wilkes, B. J., & Elvis, M. 1987, ApJ, 323, 243
Willner, S. P., Elvis, M., Fabbiano, G., Lawrence, A., & Ward, M. J. 1985, ApJ, 299, 443.